# Femtosecond pulsed laser micromachining of glass substrates with application to microfluidic devices

Malalahalli S. Giridhar, Kibyung Seong, Axel Schülzgen, Pramod Khulbe, Nasser Peyghambarian, and Masud Mansuripur

We describe a technique for surface and subsurface micromachining of glass substrates by using tightly focused femtosecond laser pulses at a wavelength of 1660 nm. A salient feature of pulsed laser micromachining is its ability to drill subsurface tunnels into glass substrates. To demonstrate a potential application of this micromachining technique, we fabricate simple microfluidic structures on a glass plate. The use of a cover plate that seals the device by making point-to-point contact with the flat surface of the substrate is necessary to prevent the evaporation of liquids in open channels and chambers. Methods for protecting and sealing the micromachined structures for microfluidic applications are discussed.

*OCIS codes:* 140.7090, 350.3850, 220.4000.

## 1. Introduction

In recent years, the availability of widely tunable femtosecond laser sources has given rise to the development of many novel microfabrication and micromachining techniques. Direct writing in bulk glass has been demonstrated, and optical components, such as waveguides and gratings, have been fabricated.[1–3] Most of these previous studies used pulses of ~100-fs duration at a wavelength $\lambda$ of ~800 nm; micromachining was then performed by tightly focusing the pulse train beneath the surface of a glass plate or substrate. Ordinary glass shows no linear absorption at the incident wavelength; however, owing to extremely high intensities at the focal point, multiphoton absorption occurs, resulting in the deposition of a large amount of energy in an extremely small volume.[4–7] This process modifies the local refractive index of the material and is exploited for fabricating waveguides and other light-manipulating devices. Recently drilling a hole through bulk glass was also demonstrated.[8]

This paper describes another application of femtosecond laser writing that is based on the ablation of substrate material at or below the surface. Instead of focusing the pulsed laser beam in the bulk of the material—as is common in the fabrication of optical waveguides and other microdevices—we typically focus the beam at or near the surface of the substrate, which results in localized ablation. By appropriately translating the substrate under computer control, we have fabricated microfluidic pathways and chambers 10–100-$\mu$m wide and 5–50-$\mu$m deep on several glass plates. Wide features are written by rastering the beam over the desired zone, whereas the depth and profile of written structures are controlled by adjusting the laser power or by multiple scanning of a given region.

In parallel with the development of sophisticated microfabrication techniques, there has been a flurry of activity relating to the so-called biochip devices for applications such as rapid on-site gene sequencing, biochemical sensing, biologically inspired computing, and biological memories.[9,10] To be successful, these devices must be compact, mass producible, flexible in their application, robust, and cost efficient. Rapid prototyping techniques play a key role in the development of such devices. A common requirement for all these devices is fast and efficient transport of biomolecules and other chemicals in the liquid phase from one location to another. Microfluidic pathways thus play a crucial role in the functioning of biochip devices. The small volume of liquids involved means that even nominal evaporation rates can cause rapid liquid loss. To prevent evaporative losses, we describe a method for covering and sealing

The authors are with the Optical Sciences Center, University of Arizona, Tucson, Arizona 85721. P. Khulbe's e-mail address is pkkhulbe@u.arizona.edu.

Received 13 September 2003; revised manuscript received 21 April 2004; accepted 21 May 2004.
0003-6935/04/234584-06$15.00/0

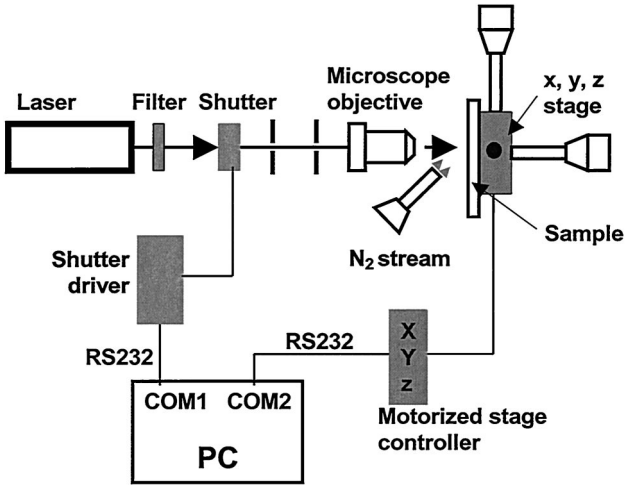


Fig. 1. Diagram of the micromachining experimental setup. The femtosecond pulsed laser is focused on the glass substrate by a microscope objective. The sample, mounted on a computer-controlled *xyz* positioner, is moved in small steps along the *x, y,* and *z* axes. PC, personal computer.

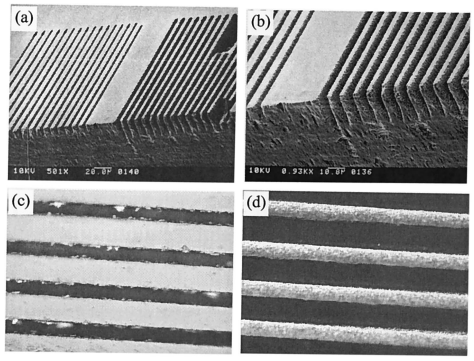


Fig. 2. Various images of micromachined channels on a glass substrate. (a) SEM image showing parallel channels written near the edge of a glass slide; the group on the right-hand side is written with a larger dose of laser pulses. The channels are ~5-μm wide and several microns deep. (b) Close-up view of the microchannels as seen through an SEM focused on the edge of the substrate. (c) Optical micrograph obtained with top illumination; the microchannels, seen as dark bands, are ~10-μm wide, with a center-to-center spacing of ~30 μm. (d) Optical micrograph of the same sample as in (c) obtained with illumination from below. The channels are seen as bright stripes on a dark background.

our micromachined structures with transparent sheets of polydimethyl siloxane (PDMS). In recent years, PDMS has been widely used in microfluidic device fabrication because of its ease of use and compatibility with biological materials.[11–14]

### 2. Experiment

Our setup is shown in Fig. 1. A train of femtosecond pulses is obtained from an optical parametric amplifier (OPA) of a Spectra-Physics laser system. The OPA is tuned to produce pulses of ~130-fs duration at a repetition rate of 1 KHz. The wavelength of the light is $\lambda = 1660$ nm, and the maximum energy per pulse is 20 μJ. When focused by a 0.25-NA infrared microscope objective, the laser beam produces a diffraction-limited spot of diameter $\sim\lambda/\mathrm{NA}$ (~7 μm) at a distance of 5 mm from the front facet of the objective lens. (The beam fills the entrance pupil of the objective.) For incident pulse energies near the maximum, the laser is intense enough to produce a bright luminescent spot caused by a breakdown of the air within the focal region.

Neutral-density filters are introduced into the beam path to attenuate the beam's intensity. The sample is mounted on a translation stage that can be moved under computer control. The computer also controls a shutter in the beam path in order to switch the beam on and off at desired locations during the writing process. Before a run begins, the sample surface is made perpendicular to the incident beam by ensuring that the retroreflected light passes through suitably positioned irises along the beam path.

### 3. Micromachining of Surface Channels

Microchannels are fabricated by focusing the beam directly on the top surface of a glass substrate (borosilicate glass or fused silica microscope slides) and then translating the substrate at ~20 μm/s. To observe the cross-sectional profile of these channels, we extend the writing all the way to one edge of the substrate. Scanning electron micrographs (SEM) and optical microscope images of typical channels are shown in Fig. 2. The cross-sectional view in Fig. 2(b) reveals the depth profile of our multiscan channels. The channel depth can be reduced by attenuating the incident beam. Wider channels can be written by scanning the beam along parallel, overlapping lines while keeping the separation between adjacent scans below the 7-μm diameter of the focused spot. The roughness of the channel sidewalls is readily visible in the optical micrographs of Figs. 2(c) and 2(d).

### 4. Chambers Connected by a Subsurface Tunnel

A unique feature of laser micromachining that is based on ablation caused by multiphoton absorption is that the ablation is tightly confined to the focal volume. Regions surrounding the focal volume are almost completely transparent to the incident radiation and remain untouched by the laser beam. We have exploited this effect and drilled a microhole through the partition wall between two adjacent microchambers, as shown schematically in Fig. 3.

The substrate used in this work was a fused-silica microscope slide. In the first step, we polished one edge of the slide (using a Logitech PM5 polishing machine) at 25 rpm for 1 h. In the second step, we machined three chambers by scanning the top surface of the substrate with the focused laser beam, as shown in Fig. 4. One of the chambers is used for calibration purposes, whereas the other two, connected by a microhole at the center of their partition wall, are used in microfluidic experiments. Each chamber is ~190 μm on the side and ~90-μm deep.

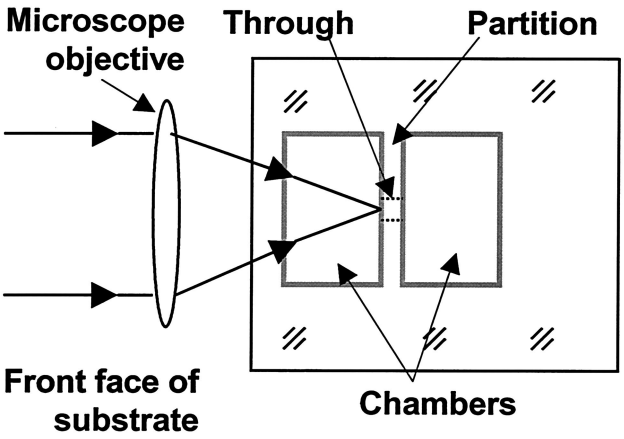


Fig. 3. Diagram showing the focusing of the laser beam through a sidewall onto the partition wall between adjacent chambers.

Two critical parameters for controlled drilling of the microhole are thickness of the partition wall (between adjacent chambers) and thickness of the outer wall (near the edge of the substrate). The outer wall, which functions as an optical window, must be smooth and homogeneous if the laser beam is to pass through it unperturbed on its way to focus at the partition wall. (We note, however, that the roughness of the inner wall perturbs the beam nonetheless.) When the outer wall was too thin, it was damaged during drilling of the microhole (exterior surface roughened) and eventually collapsed. Similarly, when the partition wall was too thin (for a given laser power), it could not withstand drilling and was demolished in the process. On the other hand, thick partition walls prevented the microhole from penetrating the entire thickness of the wall. For the cone of light emerging from the objective, the 190 μm × 190 μm size of the micro-chamber was another factor that needed consideration while optimizing the drilling process. We found the optimum thickness of the outer wall to be ~50 μm, whereas that of the partition wall was ~25 μm. Optimum conditions for writing the chambers were as follows: translation speed, ~50 μm/s; time-averaged laser power, ~18 mW; steps in the *xy* plane, ~4 μm; and steps in the depth direction, ~15 μm.

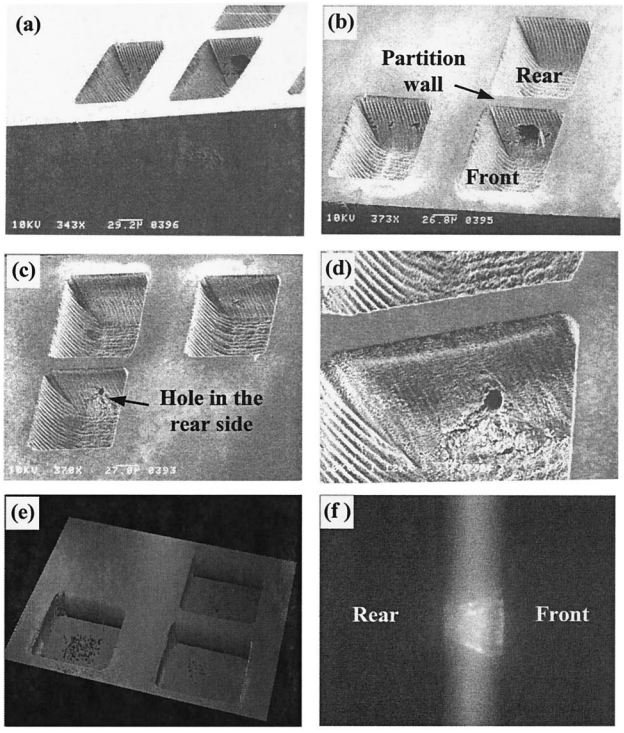


Fig. 4. Microchambers written near the edge of a glass substrate. The three chambers are ~190 μm × 190 μm × 90 μm. The wall between the two chambers on the right-hand side has been perforated with a small, conical hole. (a) View from the side showing slight damage to the front edge of the substrate through which the laser beam was focused to create the microhole. (b) Top view from the front side showing the ~40-μm-diameter opening of the microhole. (c) Top view from the rear side showing the ~15-μm diameter of the tapered hole. (d) Magnified view of the tapered end of the hole. (e) Another view of the three chambers obtained by an optical surface profiler. (f) Image of the microhole as seen through an optical microscope that looks straight at the top of the partition wall between two chambers; the tapered shape of the subsurface hole is clearly visible in this image.

In the third step the sample was turned over by 90°, and the beam was focused at the center of the partition wall between the two adjacent chambers; see Fig. 3. The microhole was drilled in the partition wall, with the beam passing through the (polished) outer wall of the chamber. After rotating the sample, we located the chambers by attenuating the beam to nonmachining intensity levels and by observing the strong scattering that occurred when the beam hit the edges of the chambers. Again, an orthogonal rastering procedure was used to drill the hole in the partition wall (translation speed, ~1–5 μm/s in the *xy* plane of the scan, with 2-μm steps in the depth direction; time-averaged laser power, ~18 mW). To prevent the debris from depositing in the chambers or surrounding areas, we exposed the substrate to a mild stream of dry nitrogen during the entire writing process. SEM and optical images of the chambers with their perforated wall are shown in Fig. 4. The microhole diameter is ~40 μm on the front side and ~15 μm on the rear side. In Fig. 4(a) the front surface of the outer wall is seen to have been slightly damaged by exposure to the laser beam during drilling. Figure 4(f) shows a cross-sectional view of the microhole as seen through an optical microscope focused under the top surface of the partition wall.

Apart from being a good demonstration of the proposed micromachining technique, the structure we have thus produced has an application to biochip devices that rely on DNA (or another polymer) translocation through nanopores. The two adjacent chambers act as the *cis* and *trans* chambers, and the lipid bilayer membrane (host to the proteinaceous nanopore) can be painted over the opening of the microhole. The conical shape of the microhole may in fact prove to be advantageous in such experiments because it might enhance the pressure gradients,

thus facilitating the passage of DNA molecules through the nanopore.

## 5. Microfluidic Structures

A potential application of femtosecond laser micromachining is direct fabrication of microfluidic pathways on glass substrates. This method can create larger and deeper surface and subsurface features than is feasible with conventional lithographic techniques. In the remainder of this paper we describe methods for fabricating sealed microfluidic pathways—as required, for instance, in practical biochip devices—and examine the microfluidic behavior inside properly sealed chambers.

We developed two methods for covering and sealing the micromachined chambers and channels produced by femtosecond laser writing. Attempts to cover these devices with flat glass plates proved futile because we failed to achieve point-to-point contact between the substrate and the cover plate owing to the roughness near the edges of the machined microstructures. We found that the liquid under the cover plate leaked out of one channel and entered adjacent channels, no matter how hard we tried to bring the two pieces of glass into perfect contact. On the other hand, PDMS material proved to be ideal for covering and sealing these microfluidic structures. In one approach we baked a sheet of PDMS and placed it directly on the top surface of the micromachined sample. Application of mild, uniform pressure over the PDMS sheet was sufficient to cause point-to-point adhesion to the surface of the substrate. In the second approach we filled the machined microstructures with photoresist (as a sacrificial filler material) and then polished the surface and proceeded to spin coat liquid PDMS on the polished substrate. After baking the sample (to solidify its PDMS cover layer), we dissolved the residual resist and removed it from channels and chambers without damaging the cover sheet (or adversely affecting the point-to-point contact between the two surfaces). Detailed descriptions of these techniques are given in the following subsections.

### A. Covering Microchannels with Preformed Polydimethyl Siloxane Sheets

PDMS (10:1 by volume of base and cross-linking agent, Sylgard 184, Dow Chemicals) was spin coated onto 2 cm $\times$ 2 cm polished Teflon substrates. We used a one-step spinning process at 1000 rpm for 60 s. Teflon was used as a substrate because it allowed easy detachment of the polymer sheet. After spin coating, the Teflon substrate was cured at 60 °C for 1 h, then a clean razor blade was used to cut out a section of the baked PDMS layer. The resulting PDMS sheet was placed over the microchannels, leaving ~1 mm from one end of the sample exposed to facilitate the insertion of a micropipette for introducing liquids into the channels. Micropipettes with outer tip diameters of less than 10 μm were drawn from glass capillary tubes by use of a commercial pipette puller (Narishige PD-5, Tokyo, Japan). The

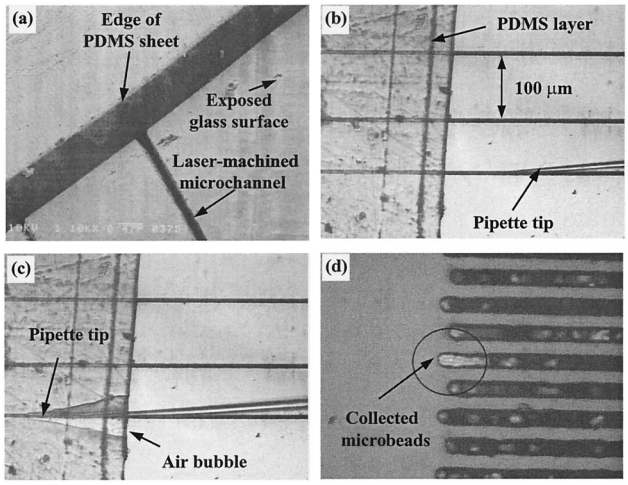


Fig. 5. PDMS-covered microchannels on a glass substrate. (a) The PDMS layer is on the left-hand side, covering part of a laser-machined microchannel; the wide, dark diagonal band is the vertical edge of the PDMS layer. (b) An array of microchannels is partially covered by a PDMS sheet, and a pipette tip is introduced into one of the channels. (c) Pushing the pipette tip under the PDMS sheet produces a small air bubble where the flexible tip (guided by the microchannel) enters the covered region. (d) Photomicrograph of the end zone of an array of microchannels covered with a PDMS sheet and filled with water. The small white particles floating in the channels are 2-μm-diameter microbeads. These microbeads were injected into the channels through a pipette, then guided to the end zone by means of a focused laser beam (optical tweezers).

pipettes were mounted on *xyz* stages and connected by flexible tubings to syringes or to a microinjector. The pipette tips were made with a slow taper, making them sufficiently flexible to help in aligning and inserting the tips into the microchannels. Figure 5 shows the process of inserting a pipette tip into a microchannel beneath the PDMS layer. An air bubble is seen to develop under the PDMS film in the vicinity of the insertion point because the small angle between the pipette and the plane of the substrate tends to lift the PDMS layer off the glass substrate. The size of the air gap thus limits the range of allowed separations between adjacent microchannels in this configuration. Figure 6 shows an array of covered microchannels that connect a microchamber (also covered) to the edge of the host substrate. In Fig. 6(d) water injected into one of the channels is seen to fill the microchamber and then return through the other channels.

### B. Spin Coating Polydimethyl Siloxane Films on Micromachined Structures

One drawback of laying down preformed PDMS sheets on micromachined structures is that very often air bubbles get trapped between the cover sheet and the substrate. If these bubbles are large enough to span the distance between the adjacent channels, they will cause fluidic cross talk between the channels. This problem is especially severe for large-area samples. Spin coating the PDMS layer directly

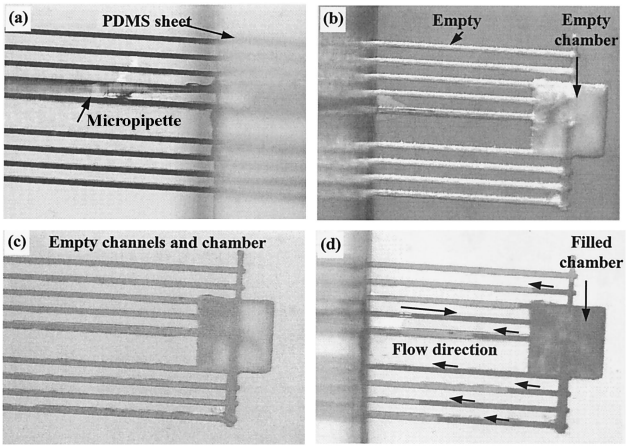


Fig. 6. A 100 μm × 100 μm × 50 μm chamber connected by nine microchannels (width, ~10 μm; depth, ~5 μm) to the edge of the host glass slide. The chamber and parts of the channels are covered with a PDMS sheet. The chamber is subsequently filled with water injected into one of the channels. (a) Photomicrograph of the bare section of the channels; a part of the (out-of-focus) PDMS sheet is also visible on the right-hand side. (b) Covered chamber and connecting channels as seen through the PDMS layer. The bare sections of the channels (seen on the left-hand side) are now out of focus. The picture, taken by illuminating the sample from below, shows the roughness of the channel walls and the uneven nature of the machined microchamber. (c) Same as (b), but illumination is from the top. (d) A microinjector sends water through a pipette inserted into the fourth channel from the top of the picture. The presence of liquid in a region (channel or chamber) makes it appear darker than the empty regions. The liquid has now filled the chamber and is returning through several of the remaining channels. In particular, the fourth channel from the bottom is filled all the way to the edge of the PDMS layer.

on the microchannels filled with sacrificial photoresist is one approach to solving the aforementioned problem. We fabricated ~1.5-mm-long surface channels running off the edge of a microscope slide (i.e., glass substrate). The machined slides were sonicated in acetone for ~30 min in order to remove any machining debris. Positive photoresist (Shipley S1813) was then spin coated on the sample at 900 rpm for 60 s. Subsequently, the slide was baked at 110 °C for 2 min. The resist formed a hard, transparent, ~50-μm-thick coating over the entire substrate, filling the channels uniformly. The coated facet was then polished with a Logitech PM5 polishing machine. A fine-finish polyutherene polishing wheel rotating at 25 rpm was used with a cerium oxide slurry (particle size ~0.5 μm). During polishing, the sample was frequently checked to avoid over polishing. (The resist had an orange tint to it, and it was possible to determine by visual inspection the point at which the resist was completely removed from the surface.) At this point the top surface of the resist-filled channels was flush with the substrate surface. Figure 7(a) is an optical micrograph of empty channels (before being filled with resist), whereas Fig. 7(b) shows the filled channels after polishing.

A PDMS solution, prepared as described in Sub-

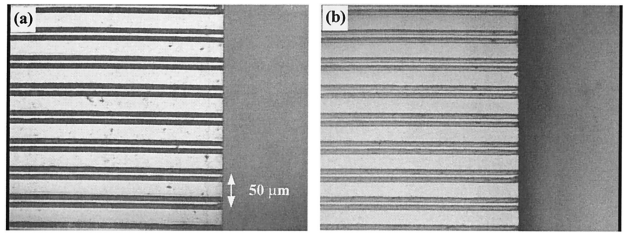


Fig. 7. (a) Micromachined parallel channels on a glass substrate. (b) Same channels after being filled with photoresist, then polished flush with the glass surface to remove debris and roughness in the areas between adjacent channels. Such polished substrates are covered with a PDMS sheet to create perfect (point-to-point) contact between the two surfaces. The resist is subsequently dissolved in acetone and removed.

section 5.A, was spin coated on the polished substrate at 900 rpm for 60 s. Following 1-h curing at 60 °C, this resulted in a 20-μm-thick PDMS film over the entire substrate. A clean razor blade was used to cut off a narrow strip of PDMS along the edge of the sample, perpendicular to the channels. This produced a step, exposing ~100 μm of the resist-filled channels. The sample was then placed vertically in a dish of continuously stirred acetone with the PDMS step fully submerged. Acetone (which does not interact with PDMS) dissolved and removed the residual resist material in the microchannels beneath the cover layer. After ~20 min in an acetone wash, the samples were coated with gold for observation under a SEM.

### 6. Flow through the Microhole in a Sealed Microfluidic Device

To observe the passage of liquids through the microhole that joins two of the three chambers of Fig. 4, we covered the sample with a 20-μm-thick PDMS sheet. The preformed PDMS film was peeled off from its Teflon backing plate and placed over the microchambers without exerting any force. To enhance the adhesion of the PDMS layer to the substrate, we baked the covered structure for an additional 3 min at 60 °C. We then inserted, by pushing from the top, two micropipettes (10-μm diameter) into the two adjacent chambers, one for injecting the deionized water and the other for extracting the trapped air; see Fig. 8. We designed the micropipette tips for sufficient stiffness by controlling the force applied during their pulling as well as the temperature used for their heating and softening. Also, for effective puncturing of the PDMS layer, we adjusted the angle between the micropipette tip and the plane of the PDMS sheet at ~45°. A microinjector was then used to fill one chamber with water by use of 60-ms, 5-psi pressure pulses. (For effective circulation, it is possible to use a vacuum pump to apply negative pressure to the pipette through which air is intended to depart, although, strictly speaking, this is not necessary.) We were thus able to observe (under a microscope) the flow of the liquid through the microhole and the sub-

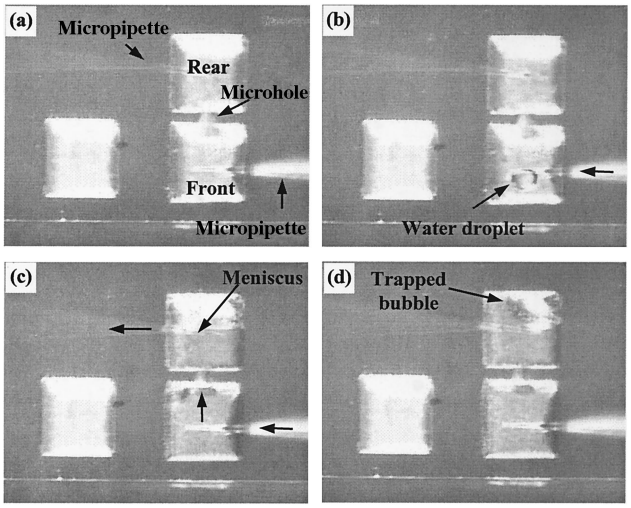


Fig. 8. Water-filling procedure for the microchambers of Fig. 4, now covered with a 20-μm-thick PDMS sheet. (a) Two micropipettes, each ~20 μm in diameter at their tapered ends, approach and puncture the top surface of the PDMS layer. (b) Deionized water is injected by a microinjector through one pipette while the air from the adjacent chamber escapes through the other. (c) Water is seen to flow between the chambers through the microhole in the partition wall. (d) Aside from a small trapped air bubble, the second chamber is filled with water. In time the bubble escapes through the second pipette, and both chambers become completely filled.

sequent filling of the adjacent chamber. A sequence of the observed events is shown in Fig. 8.

## 7. Concluding Remarks

High-power femtosecond laser pulses can be used to create microstructures at and below the surface of a glass substrate. For microfluidic applications, one can cover these structures with a PDMS sheet to protect the liquids inside the various channels and chambers and also to seal the device in order to prevent leakage and mixing of the contents of the various compartments. We described a technique for surface and subsurface micromachining of glass substrates by using tightly focused femtosecond laser pulses at a wavelength of 1660 nm. Although silicate glass is normally transparent at this wavelength, the extremely high intensity of the focused beam causes multiphoton absorption, resulting in localized ablation of the glass substrate. (Because the ablation process involves multiphoton effects, higher photon energies are preferable; in fact, most previous work in this field used laser systems operating at $\lambda \sim 800$ nm, e.g., Ti:sapphire.) Ablation is strictly confined to the vicinity of focus, leaving the rest of the substrate unaffected. We exploited this phenomenon to drill a microhole through a thin vertical wall that separates two adjacent pits machined by the same laser in a glass plate. A salient feature of pulsed laser micromachining, therefore, is its ability to drill subsurface tunnels and canals into glass substrates, a process that requires multiple steps in standard lithography. Simple microfluidic structures were fabricated on a glass plate. To prevent the evaporation of liquids in open microchannels and microchambers, we used a cover plate that seals the device by making point-to-point contact with the flat surface of the substrate. This point-to-point contact is essential if the fluids are to remain confined within their various channels and chambers on the chip without leaking into neighboring regions.

The authors are grateful to Raphael Gruener and Stephen Kuebler of the University of Arizona for illuminating discussions. This work has been supported by the Office of Naval Research Multidisciplinary University Research Initiative grant N00014-03-1-0793 and by the National Science Foundation Science and Technology Centers Program under Agreement DMR-0120967.

## References

1. K. Minoshima, A. M. Kowalevicz, I. Hartl, E. P. Ippen, and J. G. Fujimoto, "Photonic device fabrication with femtosecond laser oscillators," Opt. Photon. News **14,** 44–49 (2003).
2. K. Minoshima, A. M. Kowalevicz, E. P. Ippen, and J. G. Fujimoto, "Fabrication of coupled mode photonic devices in glass by nonlinear femtosecond laser materials processing," Opt. Express **10,** 645–652 (2002), http://www.opticsexpress.org.
3. C. B. Schaffer, A. Brodeur, J. F. Garcia, and E. Mazur, "Micromachining bulk glass by use of femtosecond laser pulses with nanojoule energy," Opt. Lett. **26,** 93–95 (2001).
4. N. Bloembergen, "Laser-induced electric breakdown in solids," IEEE J. Quantum Electron. **QE-10,** 375–386 (1974).
5. P. P. Pronko, S. K. Dutta, D. Du, and R. K. Singh, "Thermophysical effects in laser processing of materials with picosecond and femtosecond pulses," J. Appl. Phys. **78,** 6233–6240 (1995).
6. X. Liu, D. Du, and G. Mourou, "Laser ablation and micromachining with ultrashort laser pulses," IEEE J. Quantum Electron. **33,** 1706–1716 (1997).
7. C. B. Schaffer, A. Brodeur, and E. Mazur, "Laser-induced breakdown and damage in bulk transparent materials induced by tightly focused femtosecond laser pulses," Meas. Sci. Technol. **12,** 1784–1794 (2001).
8. Y. Li, K. Itoh, W. Watanabe, Kazuhiro Yamada, D. Kuroda, J. Nishii, and Y. Jiang, "Three-dimensional hole drilling of silica glass from the rear surface with femtosecond laser pulses," Opt. Lett. **26,** 1912–1914 (2001).
9. H. Bayley and P. S. Cremer, "Stochastic sensors inspired by biology," Nature **413,** 226–230 (2001).
10. E. Southern, K. Mir, and M. Shchepinov, "Molecular interactions on microarrays," Nat. Genet. **21,** 1–5 (1999).
11. P. J. A. Kenis, R. F. Ismagilov, and G. M. Whitesides, "Microfabrication inside capillaries using multiphase laminar flow patterning," Science **285,** 83–85 (1999).
12. J. C. McDonald, S. J. Metallo, and G. M. Whitesides, "Fabrication of a configurable, single-use microfluidic device," Anal. Chem. **73,** 5645–5650 (2001).
13. T. Thorsen, S. J. Maerlk, and S. R. Quake, "Microfluidic large-scale integration," Science **298,** 580–584 (2002).
14. C. Chen, D. Hirdes, and A. Folch, "Gray-scale photolithography using microfluidic photomasks," Proc. Natl. Acad. Sci. USA **100,** 1499–1504 (2003).